EPJ Web of Conferences **151**, 02003 (2017) DOI: 10.1051/epjconf/201715102003
LAM-16

Dynamic properties of liquid Ni revisited

B. G. del Rio[1,*], *L. E.* González[1], and *D. J.* González[1]

[1]Departamento de Fisica Teórica, Facultad de Ciencias, Universidad de Valladolid, Valladolid, SPAIN

Abstract. Liquid Ni has previously been studied by different approaches such as molecular dynamics simulations and experimental techniques including inelastic neutron and X-ray scattering. Although some puzzling results, such as the shape of the sound dispersion curve for $q \leq 1.0$ Å^{-1}, have already been sorted out, there still persist some discrepancies, among different studies, for greater q-values. We have performed *ab initio* simulation calculations which show how those differences can be reconciled. Moreover, we have found that the transverse current spectral functions have some features which, so far, had previously been shown by high pressure liquid metals.

1 Introduction.

Transition metals such as iron and nickel play a relevant role in geophysical science because of their presence in many planetary cores, including the Earth's core. Although iron is the dominant constituent of Earth's solid inner core and liquid outer core, however the presence of Ni (along with other light elements, i.e. sulfur, silicon) must be accounted for in order to achieve an accurate description of the different phenomena accurring in the core.

The static structure factor of liquid Ni (l-Ni) near its triple point has been measured by X-ray diffraction (XD) [1] and neutron diffraction (ND) [2, 3] techniques. As for its microscopic dynamics, the first experimental study was carried out by Johnson *et al* [4] who performed inelastic neutron scattering (INS) measurements of l-Ni at T = 1870 K and determined the dynamic structure factor, $S(q,\omega)$, within a range $2.2 \leq q \leq 4.4$ Å^{-1}. Years later, Bermejo *et al* [5] performed INS measurements of l-Ni at T= 1763 K and within the range $0.8 \leq q \leq 3.5$ Å^{-1}; therefrom, several dynamical quantities were determined. Most interesting was the dispersion relation (DR), which suggested that isothermal behaviour was attained for $q \leq 0.8$ Å^{-1}. More recently, Cazzato *et al* [6] have performed inelastic X-ray scattering (IXS) measurements on l-Ni at T= 1767 K and the $S(q,\omega)$ was determined within a range $0.2 \leq q \leq 0.8$ Å^{-1}. The associated DR was found to be rather different from the previous one, with an adiabatic dynamical regime undoubtedly holding down to at least $q \approx 0.2$ Å^{-1}.

Molecular dynamics simulations, both classical (CMD) and *ab initio* (AIMD), have also been applied to l-Ni, with most studies focused on thermodynamic states around the triple point. Among the CMD simulation studies, we mention those by Alemany

*e-mail: beatriz@metodos.fam.cie.uva.es

et al [7] and Ruiz-Martin *et al* [8] which used, in both cases, interatomic potentials constructed within the framework of the embedded atom model [9]. More recently AIMD simulation studies have been performed by Jakse *et al* [10]. These simulation studies have evaluated a range of static and dynamic properties of l-Ni and, oddly enough, they have yielded DRs very similar to each other and to the IXS data, but qualitatively different from the INS one.

Prompted by these disparities we have performed an AIMD study on several static and dynamic properties of l-Ni near its triple point. Section 2 briefly describes the theory underlying the present AIMD simulations, and section 3 reports and discusses some structural and dynamical results. Finally some conclusions are drawn.

2 Computational method.

The total potential energy of N ions with valence Z, enclosed in a volume Ω, and interacting with $N_{\rm e} = NZ$ valence electrons is written, within the Born-Oppenheimer approximation, as the sum of the direct ion-ion coulombic interaction energy, $E_{i-i}[\{\vec{R}_l\}]$, plus the ground state energy of the electronic system subjected to the ionic external potential $V_{\rm ext}(\{\vec{R}_l\})$,

$$E(\{\vec{R}_l\}) = E_{i-i}[\vec{R}_l] + E_g[n_g(\vec{r}), V_{\rm ext}(\{\vec{R}_l\})]\,, \tag{1}$$

where $n_g(\vec{r})$ is the ground state electronic density and $\vec{R}_l$ are the ionic positions. According to Density Functional Theory, $n_g(\vec{r})$ minimizes the energy functional

$$E[n(\vec{r})] = T_s[n] + E_{\rm ext}[n] + E_H[n] + E_{\rm xc}[n]\,, \tag{2}$$

where $T_s[n]$ is the non-interacting electronic kinetic energy, $E_{\rm ext}[n]$ is the electron-ion interaction energy, $E_H[n]$ is the electrostatic Hartree energy and $E_{\rm xc}[n]$ is the electronic exchange-correlation energy for which we have used the local density approximation, as parametrized by Perdew and Zunger [11]. The ion-electron interaction has been described by means of an ultrasoft pseudopotential [12].

AIMD calculations have been performed for l-Ni at a thermodynamic state near its triple point, characterized by a number density, $\rho = 0.0792$ Å^{-3} and temperature $T = 1773$ K [1]. We have used 120 atoms (i.e. $120 \times (9d{+}1sp) = 1200$ valence electrons) in a cubic supercell. After thermalization, the microcanonical AIMD simulations lasted for 21000 time steps, which amounted to 115.5 ps of simulation time. We have used a plane-wave representation with an energy cutoff of 25.0 Ryd and the single Γ point was used in sampling the Brillouin zone.

3 Results and discussion.

3.1 Static properties

The AIMD simulations provide a direct evaluation of both the pair distribution function, $g(r)$, and the static structure factor, $S(q)$. The calculated $g(r)$ (not shown) has the typical shape for a liquid, and shows a good agreement with experiment [1]. By integrating the $g(r)$ up to the position of its first minimum, $R_{\rm min} = 3.40$ Å, we have evaluated the number of nearest neighbors obtaining a value ≈ 12.6 atoms, which is typical of the simple liquid metals near their triple point [13].

Figure 1 shows the calculated $S(q)$ along with the XD [1] and ND [2, 3] data. The experimental $S(q)$'s have a symmetric main peak at $q_p \approx 3.10$ Å^{-1} and its height

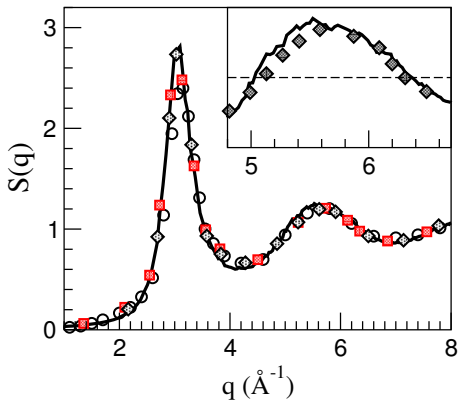

Figure 1. Static structure factor, $S(q)$, of l-Ni at T=1773 K. Full line: present AIMD calculations. Open circles: XD data from Waseda [1]. Open squares and full diamonds: ND data from Johnson *et al* [2] at T= 1875 K and Schenk *et al* [3] at T= 1765 K, respectively. The inset shows an enlarged second maximum.

varies between $S(q_p) \approx 2.4$ and ≈ 2.75 according to the XD and ND data respectively. Moreover, the ND data show a weak shoulder on the second maximum of the $S(q)$ at $q \approx 6.0$ Å^{-1}.

As evinced in Figure 1, the AIMD $S(q)$ shows good agreement with experiment; moreover, its second maximum also displays a small shoulder at $q \approx 6.0$ Å^{-1}. This type of asymmetric shape of the second peak of $S(q)$ has been experimentally observed in several liquid transition metals and it has been related to an important presence of icosahedral local order [10].

We have also estimated the isothermal compressibility, κ_T, of l-Ni by the relation $S(q \rightarrow 0) = \rho k_B T \kappa_T$ where k_B is Boltzmann's constant. The calculated $S(q)$ has been extrapolated to $q \rightarrow 0$ yielding $S(q \rightarrow 0) = 0.018 \pm 0.002$, which leads to $\kappa_T = 0.95 \pm 0.10$ (in units of 10^{11} m^2 N^{-1}) which is close to the experimental data $\kappa_T \approx 1.04 \pm 0.02$ [14].

3.2 Dynamic properties

The collective dynamics of density fluctuations in a liquid is described by the intermediate scattering function, $F(q,t)$, defined as

$$F(q,t) = \frac{1}{N} \left\langle \left(\sum_{j=1}^{N} e^{-i\vec{q}\cdot\vec{R}_j(t+t_0)} \right) \left(\sum_{l=1}^{N} e^{i\vec{q}\cdot\vec{R}_l(t_0)} \right) \right\rangle , \tag{3}$$

The Fourier Transform (FT) of the $F(q,t)$ into the frequency domain leads to the dynamic structure factor, $S(q,\omega)$, which has experimental relevance because it is directly related to the scattered intensity measured in the INS or IXS experiments. Another interesting magnitude associated with the density fluctuations is the current due to the overall motion of the particles, i.e.

$$\vec{j}(q,t) = \sum_{j=1}^{N} \vec{v}_j(t) \ \exp[i\vec{q}\cdot\vec{R}_j(t)] , \tag{4}$$

where $\vec{v}_j(t)$ is the velocity of particle j at time t. The current is usually split into longitudinal ($\vec{j}_L(q,t)$) and transverse ($\vec{j}_T(q,t)$) components with respect to $\vec{q}$. Therefrom, the longitudinal, $C_L(q,t)$, and transverse, $C_T(q,t)$, current correlation functions are obtained as

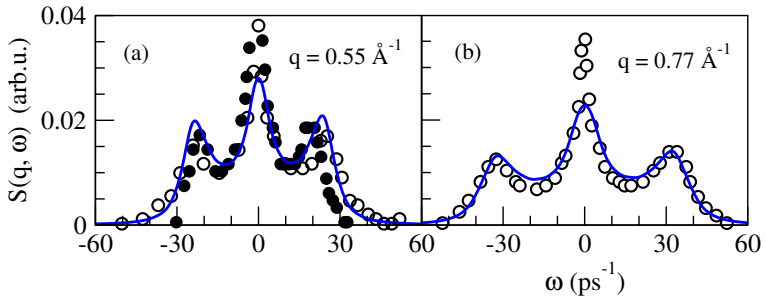

Figure 2. Dynamic structure factors, $S(q,\omega)$, of liquid Ni at T= 1773 K. (a) Filled and open circles: IXS data [6] for $q = 0.50$ and 0.60 Å^{-1} respectively. Line: AIMD results for $q = 0.55$ Å^{-1} after convolution with the experimental resolution function and inclusion of the detailed balance condition. (b) Same as before but experimental data for $q = 0.80$ and the AIMD results for 0.77 Å^{-1}.

$$C_L(q,t) = \frac{1}{N}\,\langle \vec{j}_L(q,t)\cdot\vec{j}^{\,*}_L(q,0)\rangle \qquad C_T(q,t) = \frac{1}{2N}\,\langle \vec{j}_T(q,t)\cdot\vec{j}^{\,*}_T(q,0)\rangle \quad (5)$$

The corresponding time FT give the associated spectra, $C_L(q,\omega)$ and $C_T(q,\omega)$ respectively, with $C_L(q,\omega) = (\omega^2/q^2)S(q,\omega)$.

The AIMD results for $F(q,t)$ show an oscillatory behaviour up to $q \approx (4/5)\ q_p$, with the amplitude of the oscillations becoming weaker for increasing q-values; moreover, this oscillatory shape is superposed on a rather weak diffusive component. At $q \approx q_p$, the $F(q,t)$ exhibit a slow decay, known as "de Gennes narrowing", which is induced by the strong spatial correlations at around those q-values. The AIMD $S(q,\omega)$ show side-peaks, indicative of collective density excitations, up to $q \approx (3/5)q_p$; therefrom the side- peaks evolve into shoulders lasting until $q \approx (4/5)q_p$ and for greater q's the corresponding $S(q,\omega)$ show a monotonic decreasing behavior. Figure 2 provides a comparison with the IXS data of Cazzato *et al* [6] and although it is performed for slightly different q-values, we observe a reasonable good agreement, specially concerning the position and amplitude of the side-peaks.

We have used Eqs. 4-5 to evaluate the current correlation functions $C_{L,T}(q,t)$ and their spectra $C_{L,T}(q,\omega)$. Our AIMD calculated $C_L(q,\omega)$ show one peak for each q-value and from the frequencies of those peaks, the DR for the longitudinal modes, $\omega_l(q)$, has been obtained and is plotted in Figure 3. In the figure, we have also included the experimental DRs derived from the IXS data [6], $\omega_l^{\rm IXS}(q)$, and from the INS data [5], $\omega_l^{\rm INS}(q)$.

In Ref. [6], the DR $\omega_l^{\rm IXS}(q)$ was extracted by fitting the experimental scattered intensity to an expression composed of a lorentzian (accounting for the quasielastic part) plus the damped harmonic oscillator (DHO) model (for the inelastic part). A similar procedure was applied in Ref. [5] to obtain the DR $\omega_l^{\rm INS}(q)$, although an additional lorentzian function was included to account for the incoherent part. In both cases, the frequencies assigned to the DR were the DHO frequencies obtained from the fits.

A first noticeable feature is the discrepancy between $\omega_l^{\rm IXS}(q)$ and $\omega_l^{\rm INS}(q)$ in the narrow q-region where they overlap. This was attributed by Cazzato *et al* [6] to shortcomings of the experimental INS setup at these wavevectors. Indeed, the calculated

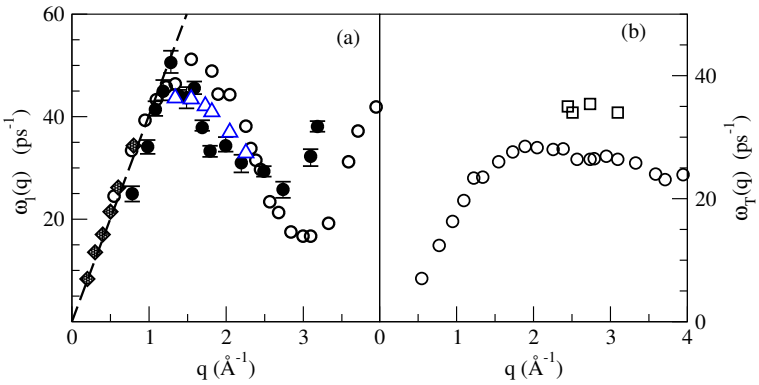

Figure 3. (a) Longitudinal DR for l-Ni at $T = 1773$ K. Circles: AIMD longitudinal DR from the positions of the peaks in the spectra $C_L(q,\omega)$. Filled circles with error bars: INS data from Bermejo *et al* [5]. Diamonds: IXS data from Cazzato *et al* [6]. Broken line: linear dispersion with the hydrodynamic sound velocity, $c_s = 4030$ m/s. Triangles: DR obtained by fitting the AIMD total (neutron weighted) dynamic structure factor to a model of two Lorentzians plus one DHO. (b) Circles and squares: AIMD transverse dispersion from the positions of the peaks in the spectra $C_T(q,\omega)$.

AIMD DR, $\omega_l(q)$, shows a good agreement with $\omega_l^{\rm IXS}(q)$. In the low-q region, the slope of the $\omega_l(q)$ curve gives a q-dependent adiabatic sound velocity which in the limit $q \to 0$ reduces to the bulk adiabatic sound velocity, c_s. We have used the AIMD results for $\omega_l(q)$, within the range $q \leq 1.0$ Å^{-1}, to evaluate its slope at $q \to 0$ and we obtained a qualitative estimate $c_s \approx 4250 \pm 150$ m/s which compares reasonably with the experimental value of $c_{s,\rm exp} \approx 4040 \pm 150$ m/s [14].

For larger q's, there is a significant difference between the $\omega_l^{\rm INS}(q)$ and the calculated AIMD $\omega_l(q)$. Moroever, as our results closely follow those obtained in CMD [7, 8] and AIMD [10] simulations, we have decided to check the accuracy of the scheme followed by Bermejo *et al* [5] to obtain their DR $\omega_l^{\rm INS}(q)$, and we applied the same procedure to out AIMD data. First, the AIMD results were used to construct the total dynamic structure factor (by weighting $S(q,\omega)$ and its self part with the corresponding coherent and incoherent neutron cross-sections of Ni). Then the total dynamic structure factor was fitted to a function comprising two Lorentzian functions for the quasielastic contributions plus a DHO model for the inelastic contribution; therefrom, the excitation frequencies of the DHO model were identified as the new calculated DR. This is also plotted in Figure 3 and it is noticed that this procedure does not reproduce the AIMD DR, $\omega_l(q)$. In fact, it yields systematically smaller frequency values which are much closer to the $\omega_l^{\rm INS}(q)$. We believe that the above results can explain the discrepancies between the INS DR, $\omega_l^{\rm INS}(q)$, and all the other DRs, either IXS or theoretical.

The transverse current spectra, $C_T(q,\omega)$, when plotted as a function of ω, may display peaks, within some q-range, which are related to propagating shear waves. From the frequencies of the peaks, a DR for the transverse modes, has been obtained and is plotted in Fig. 3. We observe two branches, a low-frequency branch whose shape is typical of simple liquid metals near melting, and a high-frequency branch, with a limited extent around q_p. The appearance of a high frequency branch is quite

unusual in monoatomic liquids. To our knowledge, it has only been found in studies performed for liquid Li, Fe and Na at high pressure [15].

4 Conclusions.

An *ab-initio* simulation method has been used to calculate some static and dynamic properties of l-Ni near its triple point. This study has been spurred by the discrepancies between the available INS and IXS measurements.

The calculated static structure factor closely follows the corresponding experimental data, including the asymmetric shape of its second peak, which has been connected to the prevalence of icosahedral short-range order.

The calculated dynamic structure factors show side-peaks indicative of collective density excitations, and they show a good agreement with the IXS data. Moreover, the calculated dispersion relation closely follows that obtained from the IXS measurements. An analysis of the modeling scheme followed to obtain the INS dispersion relation has uncovered some shortcomings which could explain its marked disparity with the IXS dispersion relation and with other simulation results.

The transverse dispersion relation shows, besides the typical low-frequency branch, a short, high-frequency one, which has not been previously found in any other monoatomic liquid metal near melting.

BGR acknowledges the financial support of Universidad de Valladolid. LEG and DJG acknowledge the support of the MECD (FIS2014-59279-P) and JCyL (VA104A11-2).

References

[1] Y. Waseda and M. Ohtani, Phys. Stat. Sol. (b) **62**, 535 (1974); Y. Waseda, *The Structure of Non-Crystalline Materials*, (New York: McGraw-Hill, 1980).
[2] M. W. Johnson, N. H. March, B. McCoy, S. K. Mitra, D. I. Page and R. C. Perrin, Philos. Mag. **33**, 203 (1976).
[3] T. Schenk, D. Holland-Moritz, V. Simonet, R. Bellisent and D. M. Herlach, Phys. Rev. Letters **89**, 075507 (2002).
[4] M. W. Johnson, B. McCoy, N. H. March and D. I. Page, Phys. Chem. Liq. **6**, 243 (1977).
[5] F. J. Bermejo, M. L. Saboungi, D. L. Price, M. Alvarez, B. Roessli, C. Cabrillo and A. Ivanov, Phys. Rev. Letters **85**, 106 (2000).
[6] S. Cazzato, T. Scopigno, S. Hosokawa, M. Inui, W. C. Pilgrim and G. Ruocco, J. Chem Phys. **128**, 234502 (2008).
[7] M. M. G. Alemany, C. Rey and L. J. Gallego, Phys. Rev. B **58**, 685 (1998).
[8] M. D. Ruiz-Martin, M. Jimenez-Ruiz, M. Plazanet, F. J. Bermejo, R. Fernandez-Perea and C. Cabrillo, Phys. Rev. B **75**, 224202 (2007); J. Non-Cryst. Solids **353**, 3113 (2007).
[9] A. F. Voter and S. P. Chen, in *Characterization of Defects in Materials*, ed. R. W. Siegel, J. R. Weertman and R. Sinclair, MRS Symposia Proceedings No 82 (Materials Research Society, Pittsburg, 1987) p. 175
[10] N. Jakse, J. F. Wax and A. Pasturel, J. Chem. Phys. **126**, 234508 (2007).
[11] D. M. Ceperly and B. J. Alder, Phys. Rev. Letters **45**, 566 (1980); J. P. Perdew and A. Zunger, Phys. Rev. B **23**, 5048 (1981).
[12] D. Vanderbilt, Phys. Rev. B **41**, 7892 (1990).

[13] U. Balucani and M. Zoppi, *Dynamics of the Liquid State*, Clarendon, Oxford, 1994.
[14] S. Blairs, Intern. Materials Rev. **52**, 321 (2007); Phys. Chem. Liq. **45**, 399 (2007).
[15] T. Bryk, G. Ruocco, T. Scopigno and A. P. Seitsonen, J. Chem. Phys. **143**, 104502 (2015) M. Marques, L. E. Gonzalez and D. J. Gonzalez, J. Phys.: Condens. Matter **28**, 075101 (2016); Phys. Rev. B **94**, 024204 (2016).